Multifractal analysis of two-dimensional carbon clusters

1993 J. Phys.: Condens. Matter 5 7087

(http://iopscience.iop.org/0953-8984/5/38/005)

J. Phys.: Condens. Matter 5 (1993) 7087–7094. Printed in the UK

Multifractal analysis of two-dimensional carbon clusters

L J Huang and W M Lau
Surface Science Western, University of Western Ontario, London, Ontario, Canada N6A 5B7

Received 25 March 1993, in final form 2 June 1993

Abstract. The multifractality of graphite and amorphous carbon fractal clusters with distinct morphologies was studied by analysing the *growth probability distribution* (GPD) using the harmonic measure. The results showed that the multifractality of the graphite clusters is similar to that of *diffusion-limited aggregation* (DLA), and that a single *phase transition* to non-multifractals occurred at a negative scaling factor, β. However, two critical points at which the multifractality was broken down were observed in the GPD of the multifractal-like amorphous carbon clusters. Such a multifractal behaviour was also found in the GPD of dissolution patterns generated by etching of porous materials, and the GPD of magnetic-microsphere aggregates, which suggests that the behaviour is common to many fractal clusters.

1. Introduction

Insights into the formation of fractal clusters can often be gained by characterizing their multifractal properties [1–2]. Multifractality of a fractal is described by the fractal measure of its *growth probability distribution* (GPD) [1–3]. Recent multifractal [4–12] analyses of *diffusion-limited aggregation* (DLA) showed that the multifractal behaviour of a DLA cluster becomes size dependent below a critical scaling factor, or in the thermodynamics terminology, below a critical inverse temperature (β_c) [4, 5]. The phenomenon is termed a *phase transition* to non-multifractals. In short, above β_c, the moment expansion shows an infinite hierarchy of phases which is the characteristic of multifractals; but below it, a single phase is present and the *free energy* [4, 5] ($F(\beta)$) of the system is no longer size independent. Such a phase transition can easily be seen in the *free energy* spectra of a DLA system either by sampling DLA clusters of different sizes, or by monitoring a single DLA cluster at different growth stages [4, 5]. The physics of the *phase transition* is attributed to the fact that the multifractal properties of a DLA at negative β are dominated by its 'fjords', where the growth probability approaches a minimum value. During the evolution of a DLA cluster, the fjords become more and more heavily screened from growth. The screening eventually leads to the breakdown of the multifractality of the DLA cluster.

For a real physical system, especially for fractal clusters observed in thin solid films [13–16], on which this paper is based, an infinite scaling regime cannot usually be found experimentally for either the imperfection of the detection tools or the intrinsic *cut-off* in the system [17]. In addition, the scaling regime for the fractal clusters observed in most of the thin solid films was limited by the linear size of the clusters. Nonetheless, it is expected that more geometrical information of the cluster can be revealed and be distinguished using the multifractal approach than using the description of a single fractal dimension. In this paper, we discuss the multifractality of fractal clusters of two distinct morphologies and the corresponding geometrical properties.

0953-8984/93/387087+08$07.50

2. Experimental details

The samples employed in the present study were ultra-thin films consisting of 10–20 nm thick graphite clusters mosaiced or inlaid with less than 10 nm thick amorphous carbon. The films were prepared by filament-assisted chemical vapour deposition. In this experiment, a tungsten filament was heated to about 2000 °C to decompose a 0.5% methane/hydrogen gas mixture above a silicon substrate at 1000 °C. After the deposition, the silicon substrate was removed by etching in an HF/HNO_3 solution and the thin carbon film was floated onto a typical 3 mm grid for transmission electron microscopic (TEM) analysis. An Hitachi H800 microscope with an electron beam of 150 keV was used for the structural analysis. An example of the TEM image of this sample structure is shown in figure 1(*a*). Secondary electron microscopic analysis of the region of the same carbon foil underneath the locations of the grid lines showed that many of secondary electrons emitted from the grid were transmitted through the foil. Therefore, the graphite thickness was estimated to be 10–20 nm. The results from the transmission electron diffraction in a selected area mode, as shown in the inset of figure 1(*a*), indicated that the graphite was (0001) oriented. Since the cluster size is much larger than its thickness, the growth was almost two dimensional along the basal plane. Diffraction analysis also showed that the regions between the graphite clusters were amorphous. Furthermore, x-ray photoemission spectroscopic analysis of the foil showed the presence of only carbon; hence these regions were identified as amorphous carbon. The brightness contrast between the graphite and the amorphous carbon suggests that the amorphous carbon was thinner than 10 nm. Although the present analysis could not determine whether the graphite clusters were mosaiced with or inlaid on amorphous carbon, the two phases were definitely joined, otherwise the graphite clusters would have fallen apart. In the following analysis, a mosaic structure was assumed.

3. Analysis approach

In experimental measurement of the multifractality of a fractal cluster, it is essential to measure its GPD. Since monitoring the growth of a fractal cluster in solid state with time evolution to determine GPD directly ('natural measure') is often technically difficult, an alternative approach (harmonic measure) previously proposed by Hayakawa *et al* [18] is frequently employed. Both these two measures were applied to calculate the multifractal properties of an experimentally grown fractal-like cluster, and the validity of using the harmonic measure when the 'natural measure' is not available was shown by Ohta and Honjo [19]. The principle of the harmonic measure rests on the fact that random diffusion satisfies the Laplace equation and that the growth probability, p_i, of the fractal cluster at time t and a growing site r_i is proportional to the Laplacian field strength ($|\nabla_n \phi(r_i, t)|$), i.e., $p_i(r_i, t) \propto |\nabla_n \phi(r_i, t)|$. In other words, the Laplacian potential distribution of the cluster probes the geometry of the cluster and correlates it to the kinetic properties of the cluster. Therefore, the GPD can be recovered from the analysis of a static cluster, which can then be used to calculate the multifractal properties of the cluster. In practice, since only static clusters are analysed, the system size cannot be used directly as the scaling factor. Instead, the GPD is divided into subsets. Each subset lies within a box of length b, and the measure of each subset is $p_i(b)$. This is done by covering the GPD with a grid of boxes of length b, then measuring the sum of the occupied sites inside the box [3, 12]. For an object with self-similarity, variation of the box size b is equivalent to variation of the system size L. Therefore, the multifractality of the cluster can be described by the probability measure

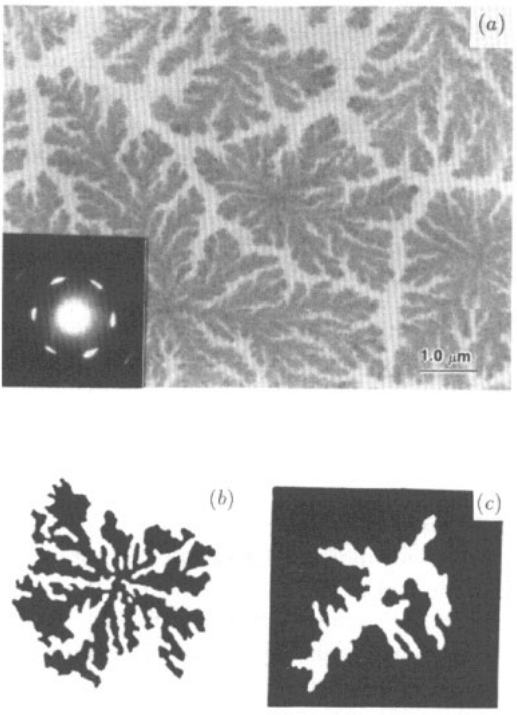

Figure 1. A TEM image (×5000) of (*a*) the mosaic fractal-like pattern used in the present study, (*b*) a typical graphite cluster, and (*c*) a typical amorphous cluster. (The dark area is contributed by graphite and the bright area by amorphous carbon.)

$p_i(b)$ on the condition that $b \ll L$. In this approach, it is convenient to define an effective size, $l = L/b$. Theoretically, the multifractal formalism is established at the limit $l \to \infty$ (either $L \to \infty$ or $b \to 0$). In practice, the limits of b can be set at an experimental *cut-off* where $p_i(b)$ is trivial, and such a b will not introduce new breakdowns in the corresponding measure [20].

As discussed above, it is expected that the harmonic measure is not universal for retrieving kinetic information of distinct fractal clusters formed with diverse kinetics. For example, it cannot be used to recover the real GPD of fractal clusters formed via cluster–cluster aggregation. Nevertheless, the approach is valid for probing the geometrical properties of static fractal clusters, since the growth probability of the probing particle at the surface of each distinct cluster is uniquely determined by the local Laplace field and hence the geometry of the cluster itself. When it happens, the simulated GPD would be the 'nominal' GPD which carries only the geometrical information of the cluster.

In the actual analysis, a total of 27 clusters were selected from different parts of the films for analysis of each morphology. Typical clusters of graphite and amorphous carbon are shown in figure 1(*b*) and (*c*), respectively. As we have reported in a previous publication [16], the fractal dimensions of individual clusters grown in the same solid film depended on the local conditions and its multifractal spectra could therefore be different from one another. In order to eliminate such an error in later averaging, the 27 clusters for analysis were chosen following the condition that the difference between the measured fractal dimension of each chosen cluster and that of the average was less than ± 0.10.

The TEM images of the observed clusters were digitized with a Mackintosh computer

system and a Hewlett Packard laser scanner with a 300 × 300 pixel matrix and an appropriate contrast threshold to separate pixels belonging to a cluster from those in the background. The discrete Laplace equation of the two-dimensional square matrix was solved with the free-boundary condition by the relaxation method. The calculated GPD was then covered by a grid of boxes of length b on the lattice. The measure $p_i(b)$ was then obtained by counting the occupied pixels within each box ($\sum_{\text{box}} p_i$) and normalized with $\sum_i p_i(b)$. The 'partition function', $Z(\beta, l)$, was estimated by [3–5]

$$Z(\beta, l) \equiv \sum_i (p_i(b))^\beta \simeq A(\beta, l)(l)^{-F(\beta)} \tag{1}$$

where β is the multifractal scaling factor, or in the equivalent thermodynamics terminology, the inverse temperature. The free-energy spectrum, $F(\beta, l)$ was then calculated by the following equation:

$$F(\beta) = \lim_{l\to\infty} F(\beta, l) \equiv \lim_{b\to 0}[-\log Z(\beta, l)/\log b]. \tag{2}$$

Finally, the generalized fractal dimension was obtained by $D(\beta) = F(\beta)/(\beta - 1)$.

The morphology of the cluster shown in figure 1(b) is similar to those of the computer-simulated fractal clusters [21], while that of the cluster shown in figure 1(c) is similar to that of the 'chemical dissolution pattern' reported by Daccord [22]. Several factors, such as diffusion, successive nucleation, growth of the crystallites at the interface, and diffusion-limited branch enlargement, may have been involved in such non-equilibrium solid-state processes [23, 24]. In the following discussion, only the geometrical characteristics of the clusters are addressed.

4. Results and discussion

Figure 2 shows the scaling regime for the two clusters shown in figure 1(b) and (c), respectively. The data shown were from the box-counting approach, $N \propto b^{-D(0)}$, and the end of linearity of the data for the two different clusters is indicated by $b_{\max}$ and $b'_{\max}$, respectively. In these two cases, $L/b_{\max}$ was about 2.24 for graphite clusters and about 1.78 for amorphous carbon clusters. From the data, the $D(0)$ for the graphite clusters (figure 1(b)) was determined to be 1.68 ± 0.08 which is only marginally smaller than that of a DLA cluster. As such, the result suggests that the geometry of the graphite cluster can be approximated by DLA with a sticking probability of slightly less than unity [13]. The breakdown in the multifractal free-energy spectrum of a DLA cluster below a negative inverse temperature was also observed, as shown in figure 3(a). The breakdown can be further manifested by defining the following free-energy fluctuation function:

$$\Delta\Phi(\beta) = F(\beta, l_{\min}) - F(\beta, l_{\max}) \tag{3}$$

where $l_{\max}$ and $l_{\min}$ are, respectively, the maximum and minimum box size used in this study. The results (figure 3(b)) clearly show that such a free-energy fluctuation was near zero when $\beta > \beta_c \simeq -1$. In the regime of $\beta < 0$, the free energy is dominated by the minimum growth probability, $p_{\min}$, or the $E_{\max}$ ($E_{\max} \equiv -\ln p_{\min}/\ln l$) of the cluster. Therefore, determination of the scaling forms of the minimum growth probability bears some importance when the multifractal breaks down into a single phase. It has been shown that the dependence of $p_{\min}$ on L may take an exponential or power-law form [5–12]. In the

present study, the E_{max} measured for the graphite clusters fitted well into the relation [5, 6] $E_{max} \propto l^2/\ln l$ (with a correlation coefficient of 0.985 ± 0.021 for all the clusters sampled). This result again has been shown to be the characteristics of a DLA cluster. These results are qualitatively the same as those obtained from DLA clusters of different sizes. Such an agreement confirms the validity of the present approach in using the Laplacian field strength for the determination of GPDs and using the box size as the multifractal scaling factor for measuring multifractal properties.

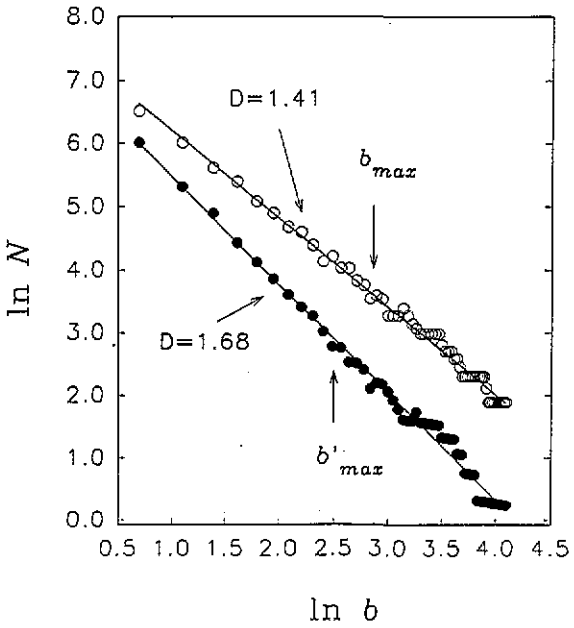

Figure 2. Fractal dimensions for the graphite cluster shown in figure 1(*b*) (filled circles) and the amorphous cluster shown in figure 1(*c*) (open circles). the data were obtained using the box-counting approach by varying the box size *b*.

To examine whether the above results were due to statistic fluctuations, averaging was performed among the clusters with the same morphology and fractal dimensions ($D_i(0) - \bar{D}(0) < \pm 0.1$). The results are listed in table 1, which clearly shows that the divergence of the multifractal spectra of these clusters is intrinsic.

In contrast to the graphite clusters, the multifractal analysis of a typical amorphous carbon cluster (figure 1(*c*)) showed that the fractal dimension was 1.41 ± 0.04, which is much smaller than that of a DLA cluster. It is more interesting that the free-energy spectrum, as shown in figure 4(*a*), diverged not only below a negative β but also above a positive β. The two transition critical points β_c^- and β_c^+ in the free-energy spectra are more clearly seen in the free-energy-fluctuation plot (figure 4(*b*)) from which $\beta_c^- = -1$ and $\beta_c^+ = 3$ can be determined. The breakdown of multifractality above a positive β, a 'temperature domain' where the 'tips' of a DLA-like cluster will dominate the multifractal properties of the cluster, can be understood by a qualitative examination of the cluster geometry as shown in figure 1(*c*). The amorphous carbon cluster, in comparison to the graphite cluster, is of an open structure with less tip splitting. Only large fingers have been developed which implies a screening of the development of small fingers (the 'tips'). In addition, the dependence of

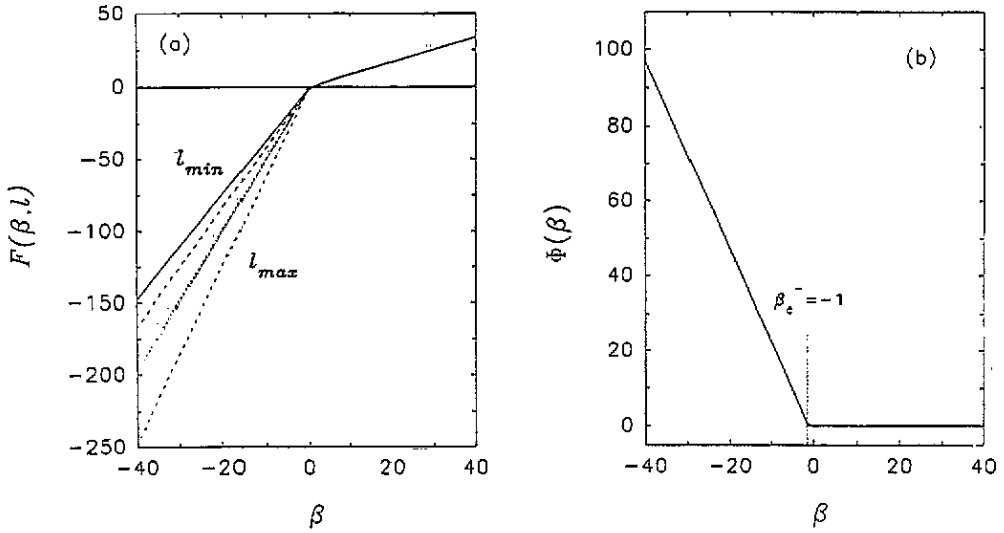

Figure 3. Analysis of the free energy of the graphite cluster: (*a*) the free-energy spectra with varying box sizes ($l_{max} = 10^2/2$, $l_2 = 10^2/3$, $l_3 = 10^2/4$, $l_4 = 10^2/5$, $l_5 = 10^2/7$, and $l_{min} = 10^2/11$); (*b*) the free-energy fluctuation with respect to l.

Table 1. List of the multifractal spectrum parameters averaged over different clusters.

Clusters averaged	$F(l_{min}) - F(l_{max})$ $\beta = -40$	$\beta = +40$	β_c^-	β_c^+
Clusters type I ($D(0) \simeq 1.68$)				
1	97	0	−1	—
10	86	0	−0.9	—
20	92	0	−1	—
27	90	0	−0.9	—
Cluster type II ($D(0) \simeq 1.41$)				
1	58	6.6	−1.0	3.0
10	50	5.3	−0.8	2.4
20	46	5.8	−0.9	2.9
27	49	6.1	−1.1	2.7

the E_{max} on l of the amorphous carbon cluster at a negative temperature was found to have the following scaling form:

$$E_{max} \propto l^2/(\ln l)^2 \tag{4}$$

or $p_{min} \propto \exp(-Al^2/\ln l)$, where A is a proportionality constant. As such, E_{max} of the amorphous carbon cluster behaved quite differently from E_{max} of the graphite cluster. The analysis of the dependence on l of the growth probability of the amorphous carbon cluster at $\beta > \beta_c^+$ showed that $p_{max} \propto \exp(-Al^2)$ or $E_{min} \propto l^2/\ln l$. Hence, E_{min} of the amorphous carbon cluster had a similar behaviour to that of E_{max} of the graphite cluster. In other words, the screening of the 'tips' of the amorphous carbon clusters from further growths is

similar to the screening of the 'fjords' of the graphite clusters. In figure 1(*c*), the screening of the 'tips' of the amorphous carbon clusters is illustrated by the large fingers and few tip splittings of the fingers. Similar effects of averaging over different clusters can also be found in table 1.

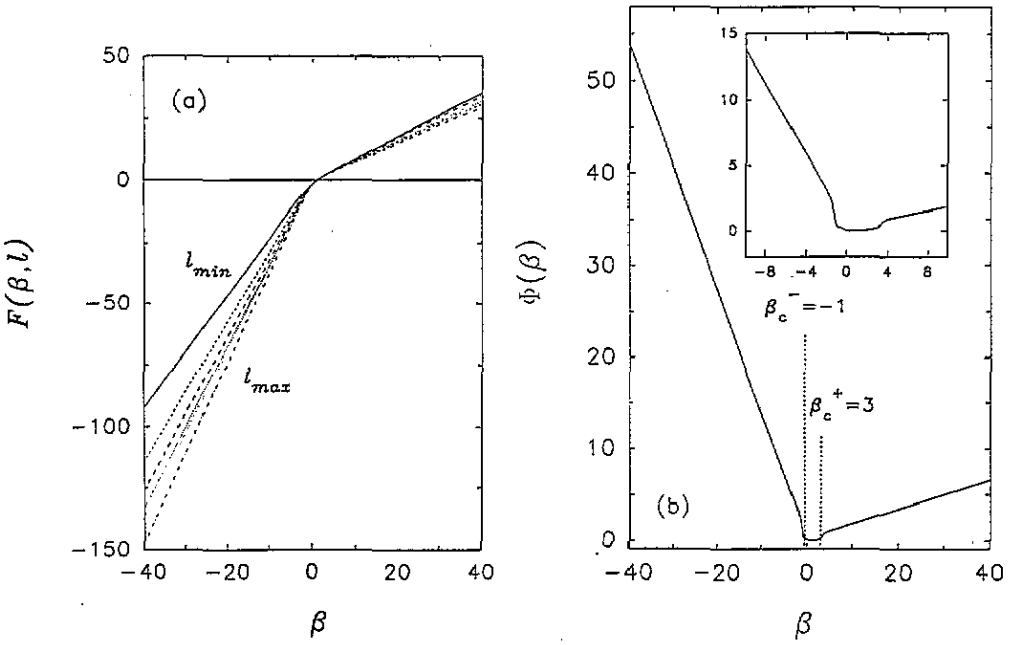

Figure 4. Analysis of the free energy of the amorphous carbon cluster: (*a*) the free-energy spectra with varying box sizes (labelling scheme the same as that in figure 3); (*b*) the free-energy fluctuation with respect to l.

As we have mentioned earlier in this paper, it is difficult to obtain the kinetics for the formation of the amorphous carbon clusters by simply comparing the results to those from the existing models. For example, the less frequent tip splitting and enlarged branches of the 'chemical dissolution pattern' in porous media were modelled by Daccord using a '*cumulative* DLA model'. The simulated results recovered the observed morphology of the 'dissolution patterns' and a low fractal dimension of 1.43 was found. However, such a process is at least not experimentally evident to have been involved in the formation of the clusters in the present observations, although the morphology and the fractal dimension were similar.

The implication of the fact that the free energy of the amorphous carbon cluster is size independent only in a limited range of scaling factor β goes beyond the nature of the cluster production in the present study. Similar multifractal properties are also expected from other multifractal-like clusters. For example, since the fractal dimension of the amorphous carbon is very close to that of a dissolution pattern generated from etching a porous material, multifractal analysis was applied to such a pattern previously reported by Daccord [22]. Similarly to the results on the amorphous carbon cluster, the dissolution pattern gave a size-independent free energy only in a narrow β range with a breakdown at both negative and

positive β. In addition, the lack of tip splitting in the growth of the iron-oxide magnetic-microsphere aggregates [16] also results in the divergence of their multifractal spectra at both negative and positive β.

5. Conclusions

In conclusion, we show that the geometry of the two kinds of cluster with distinct morphologies can be clearly described by their multifractality. Divergency of the multifractal spectra in both positive and negative regions of β was found for the carbon clusters discussed here.

Acknowledgments

The authors would like to acknowledge financial support from the Natural Sciences and Engineering Council of Canada and from Surface Science Western.

References

[1] Halsey T C, Jensen M H, Kadanoff L P, Procaccia I and Shraiman B I 1986 *Phys. Rev.* A **33** 1141
[2] Paladin G and Vulpiani A 1987 *Phys. Rep.* **156** 147
[3] It has been shown that caution must be taken in measurement of $f(\alpha)$ from a static cluster: see, e.g., Blunt M 1989 *Phys. Rev.* A **39** 2780
[4] Lee J and Stanley H E 1988 *Phys. Rev. Lett.* **61** 2945
[5] Blumenfeld R and Aharony A 1989 *Phys. Rev. Lett.* **62** 2977
[6] Schwarzer S, Lee J, Bunde A, Havlin S, Roman H E and Stanley H E 1990 *Phys. Rev. Lett.* **65** 603
[7] Schwarzer S, Lee J, Havlin S, Stanley H E and Meakin P 1991 *Phys. Rev.* A **43** 1134
[8] Mandelbrot B B and Evertsz C J G 1990 *Nature* **348** 143
[9] Mandelbrot B B and Vicsek T 1989 *J. Phys. A: Math. Gen.* **20** L377
[10] Harris A B and Cohen M 1990 *Phys. Rev.* A **41** 971
[11] Trunfio P and Alstrom P 1990 *Phys. Rev.* B **41** 896
[12] Ball R and Blunt M 1989 *Phys. Rev.* A **39** 3591
[13] Elam W T, Wolf S A, Sprague J, Gubser D U, Vechten D, Barz G L and Meakin P 1985 *Phys. Rev. Lett.* **54** 701
[14] Niklasson G A, Torebring A, Larsson C, Granqvist C G and Farestam T 1988 *Phys. Rev. Lett.* **60** 1735
[15] Huang L J, Ding J R, Li H D and Liu B X 1988 *J. Appl. Phys.* **63** 2879
[16] Huang L J, Liu B X, Ding J R and Li H D 1989 *Phys. Rev.* B **40** 858
[17] For example, the *cut-off* in [15] is the size of the grains which aggregated into the cluster.
[18] Hayakawa Y, Sato S and Mutsushita M 1987 *Phys. Rev.* A **36** 1963
[19] Ohta S and Honjo H 1988 *Phys. Rev. Lett.* **60** 611
[20] See, e.g., Jensen M H, Paladin G and Vulpiani A 1991 *Phys. Rev. Lett.* **67** 208. The cut-off imposed on the weights of the elements of a partition of the multifractal set in the present work was from 10^{15} to 10^{-4}. No breakdown in the free energy spectra at $\beta > 0$ due to the cut-off was found.
[21] Meakin P 1983 *Phys. Rev.* A **27** 1495
[22] Daccord G 1987 *Phys. Rev. Lett.* **58** 479
[23] Alexander S, Bruinsma R, Hilfer R, Deutscher G and Lereah Y 1988 *Phys. Lett.* **60** 1514
[24] Wang D M, Zhao Y D and Wu Z Q 1992 *J. Appl. Phys.* **71** 5904